



Published in final edited form as:

*Biochemistry*. 2009 December 15; 48(49): 11773–11785. doi:10.1021/bi901326k.

## THE MOLECULAR BASIS OF ASSOCIATION OF RECEPTOR ACTIVITY-MODIFYING PROTEIN 3 WITH THE FAMILY B G PROTEIN-COUPLED SECRETIN RECEPTOR#

Kaleeckal G. Harikumar, John Simms, George Christopoulos, Patrick M. Sexton, and  
Laurence J. Miller\*

Department of Molecular Pharmacology and Experimental Therapeutics, Mayo Clinic, Scottsdale, AZ 85259; Drug Discovery Biology Laboratory, Monash Institute of Pharmaceutical Sciences and Department of Pharmacology, Monash University, Melbourne 3800, Australia

### Abstract

The three receptor activity-modifying proteins (RAMPs) have been recognized as being important for the trafficking and function of a subset of family B G protein-coupled receptors, although the structural basis for this has not been well established. In the current work, we use morphological fluorescence techniques, bioluminescence resonance energy transfer, and bimolecular fluorescence complementation to demonstrate that the secretin receptor associates specifically with RAMP3, but not with RAMP1 or RAMP2. We use truncation constructs, peptide competition experiments, and chimeric secretin-GLP1 receptor constructs to establish that this association is structurally-specific, dependent on the intramembranous region of the RAMP and TM6 and TM7 of this receptor. There were no observed changes in secretin-stimulated cAMP, intracellular calcium, ERK1/2 phosphorylation, or receptor internalization in receptor-bearing COS or CHO-K1 cells in the presence or absence of exogenous RAMP transfection, although the secretin receptor trafficks normally to the cell surface in these cells in a RAMP-independent manner, resulting in both free and RAMP-associated receptor on the cell surface. RAMP3 association with this receptor was shown to be capable of rescuing a receptor mutant (G241C) that is normally trapped intracellularly in the biosynthetic machinery. Similarly, secretin receptor expression had functional effects on adrenomedullin activity, with increasing secretin receptor expression competing for RAMP3 association with the calcitonin receptor-like receptor to yield a functional adrenomedullin receptor. These data provide important new insights into the structural basis for RAMP3 interaction with a family B G protein-coupled receptor, potentially providing a highly selective target for drug action. This may be representative of similar interactions between other members of this receptor family and RAMP proteins.

---

Receptor activity-modifying proteins (RAMPs) are type I single transmembrane proteins that associate with a subset of G protein-coupled receptors (GPCRs), thereby having the potential to affect their ligand binding specificity and affinity, signaling, and trafficking (1). In addition to these potential functional effects, RAMP-GPCR association has been proposed to represent

---

#This work was supported by grants from the National Institutes of Health, DK46577 (LJM), the National Health and Medical Research Council of Australia (NHMRC), 436781 and 519461 (PMS) and from the Fiterman Foundation (LJM). PMS is a Principal Research Fellow of the NHMRC.

\*Address for all the correspondence to: Mayo Clinic 13400 East Shea Blvd Scottsdale, AZ 85259 Tel.: (480) 301-6650, Fax: (480) 301-6969 miller@mayo.edu.

**Supporting Information Available.** Supplemental data are available that show the alignment of the sequences of the human secretin and GLP1 receptors that was utilized to determine the sequences of the chimeric receptor constructs used in the current report. This material is available free of charge via the Internet at <http://pubs.acs.org>

an opportunity for the development of highly selective ligands that target this interface, providing an opportunity to achieve a greater degree of selectivity than those drugs that target only the particular GPCR molecule (2). However, little is currently understood regarding the molecular basis of RAMP association with GPCRs or the structural characteristics of the shared interface between these molecules.

The RAMPs are a family of three proteins, RAMP1, RAMP2, and RAMP3, having approximately 30 percent amino acid conservation. Each has a relatively large extracellular amino-terminal region, a single transmembrane segment, and a small intracellular carboxyl-terminal tail, with RAMP1 and RAMP3 approximately 148 amino acids in length, and RAMP2 having an additional 26 amino acids (3). RAMPs were first identified when they were found to be responsible for the translocation of the calcitonin receptor-like receptor (CLR) from the biosynthetic compartments (endoplasmic reticulum and golgi) of the cell to the plasma membrane (4). Of note, both this receptor and the RAMPs are expressed relatively poorly on the cell surface in the absence of an appropriate partner molecule. The ability of interacting GPCRs to enable translocation of RAMPs to the cell surface has become a key feature utilized in exploring their spectrum of association with other receptors. However, it is particularly noteworthy that there are currently only a small number of receptors recognized as interacting with RAMPs, yet RAMPs are expressed in many tissues in which these receptors are absent. Clearly, more information is needed regarding the basis of RAMP association with other molecules.

The specific RAMP association with CLR determines its pharmacology. RAMP1/CLR is phenotypically a calcitonin gene-related peptide (CGRP) receptor; RAMP2/CLR and RAMP3/CLR exhibit adrenomedullin receptor phenotypes (5). Similarly, RAMP association with the calcitonin receptor is necessary to express its amylin receptor phenotype (6). Other family B GPCRs, such as PTH1, PTH2, VPAC1, and glucagon receptors may associate with RAMPs, but to date no effects on their pharmacological profiles have been reported (7). Of interest, the VPAC1 receptor can associate with all three RAMPs, while the PTH1 and glucagon receptors associate only with RAMP2 and the PTH2 receptor associates only with RAMP3 (7,8). Other family B GPCRs, like the VPAC2, GHRH, GLP1 and GLP2 receptors have not been found to associate with RAMPs (8). A recent study shows that RAMP1 and RAMP3 can also effectively interact with the Family C calcium-sensing receptor, where they facilitate receptor glycosylation and its efficient delivery to the cell surface (9).

In the current work, we identified a new, previously-unrecognized RAMP3-specific interaction with another family B GPCR, the secretin receptor, and have explored the molecular basis for this association. This receptor was the first family B GPCR to be isolated, and has been extensively studied as a prototypical member of this receptor family (10). It is physiologically important as a mediator of pancreatic and biliary alkaline secretion that is critical for normal digestion (11). Our experience in working with this receptor, providing extensive insights into its structure (12,13) and into the molecular basis of its constitutive dimerization (14-18), provide substantial insights into its function and key resources to explore the basis of its RAMP association. In the current project, we have utilized fluorescence, resonance energy transfer, and morphological techniques to establish the presence of a structurally-specific association between RAMP3 and the secretin receptor, and have localized the basis of this interaction to an intramembranous region of the RAMP and specifically to TM6 and TM7 of this receptor.

## EXPERIMENTAL PROCEDURES

### Receptor constructs

RAMP constructs fused in-frame at their carboxyl terminus with *Renilla* luciferase (Rlu) or yellow fluorescent protein (YFP) were prepared using GATEWAY technology from

Invitrogen (Carlsbad, CA). The cDNAs encoding each human RAMP (RAMP1, RAMP2 and RAMP3) were amplified with Expand High Fidelity Enzyme blend (Roche) using a forward primer that introduced four nucleotides (CACC) immediately before the ATG initiation codon and a reverse primer that removed the receptor's natural stop codon. The PCR products were subcloned into the pENTR/D-TOPO vector using the pENTR directional TOPO Cloning Kit (Invitrogen), following the manufacturer's recommendations. The destination vectors were generated using the GATEWAY Vector conversion system, as previously described (15). The recombination reactions between pENTR-specific receptor cDNA and the destination vectors (pCR3.1-Rlu-dest and pEYFP-N1-dest) were performed using the LR recombinase kit. Additional RAMP constructs were prepared by inserting the amino- or carboxyl-terminal YFP fragments, YFP(1-158) (YN) or YFP(159-238) (YC), respectively, into the BglII/HindIII restriction sites before the TGA stop codon. The  $\Delta(10-100)$  RAMP3 construct was created by inserting two XbaI sites after the relevant codons using the QuikChange site-directed mutagenesis kit (Stratagene, La Jolla, CA). The nucleotide sequence between these sites was excised to yield RAMP3 sequences lacking 90 amino acids.

Amino- and carboxyl-terminal-truncated secretin receptor constructs, Rlu- and YFP- tagged human secretin receptor (SecR) constructs, the CLR receptor construct, and an Rlu- tagged CTR construct have been prepared previously (16,18). Cmyc-tagged secretin receptor was prepared by primer extension PCR. cDNAs for N-ethylmaleimide-sensitive factor (pCMV6-NSF) and sodium-hydrogen exchange regulatory factor (pCMV6-NHERF1) were purchased from Origene (Rockville, MD). The secretin receptor mutant in which Gly<sup>241</sup> within TM4 was replaced with Cys (G241C) was prepared by oligonucleotide-directed mutagenesis. All sequences were confirmed by direct DNA sequencing.

Chimeric secretin-GLP1 receptor constructs were prepared by fusion of complementary fragments of the two receptors, replacing segments of the secretin receptor with corresponding segments of the GLP1 receptor, again verifying the resulting sequences. Constructs consisted of the following: (SecR<sub>1-124</sub>)(GLP1R<sub>121-230</sub>)(SecR<sub>223-419</sub>) substituting the TM1-TM3 region of the secretin receptor with the corresponding region of the GLP1 receptor, denoted Sec (GLP1<sub>TM1-3</sub>)R; (SecR<sub>1-230</sub>)(GLP1R<sub>232-311</sub>)(SecR<sub>302-419</sub>) substituting the TM4-TM5 region of the secretin receptor with the corresponding region of the GLP1 receptor, denoted Sec (GLP1<sub>TM4-5</sub>)R; and (SecR<sub>1-309</sub>)(GLP1R<sub>319-388</sub>)(SecR<sub>377-419</sub>) substituting the TM6-TM7 region of the secretin receptor with the corresponding region of the GLP1 receptor, denoted Sec(GLP1<sub>TM6-7</sub>)R. Each of these constructs expressed in intact cells was shown to bind secretin and to signal normally, establishing their abilities to be synthesized and to traffick normally to the cell surface where their architecture was intact and able to couple with G<sub>s</sub> (see data below).

## Peptides

Synthetic peptides corresponding to each of the predicted transmembrane segments of the human secretin receptor were synthesized as described previously (17). This was achieved by manual solid-phase techniques using Pal resin (Advanced Chem Tech) and Fmoc-protected amino acids. The peptides were purified to homogeneity using reversed-phase HPLC with an octadecylsilane reversed-phase column. Resulting peptides had their identities verified by mass spectrometry. For use, they were solubilized in dimethyl sulfoxide (DMSO) prior to dilution with KRH medium to yield a final concentration of 0.1% DMSO, with this concentration of DMSO shown to have no effect in the relevant assays.

## Cell culture and transfection

African green monkey kidney (COS) cells obtained from the American Type Culture Collection (ATCC) (Manassas, VA) were propagated in tissue culture plasticware in Dulbecco's Modified Eagle's Medium (DMEM) (Invitrogen, Carlsbad, CA) supplemented

with 5 % Fetal Clone II (Hyclone laboratories, Logan, UT) in a humidified environment including 5 % CO<sub>2</sub>. They were passaged approximately twice per week. For interaction studies, cells were transfected using the modified diethylaminoethyl (DEAE)-dextran method (17) and were studied approximately 72 h after transfection. For functional studies, COS cells were seeded at a density of 30,000 per well in a 96-well plate using DMEM supplemented with 10 % (v/v) Fetal bovine serum (FBS) 24 h prior to transfection. Transfection of cmyc-tagged secretin receptor, RAMPs, NSF, and NHERF1 plasmids was performed according to cell type-specific recommendations in the Metafectine transfection reagent manual (Biontex Laboratories, GmbH). Chinese hamster ovary (CHO) K1 cells (American Type Culture Collection) were cultured in complete media (5 % FBS, DMEM) and seeded into 75 cm<sup>2</sup> culture flasks to achieve approximate 90 % cellular confluency the next day. These cells were then transfected with cmyc-secretin receptor and human RAMP1, RAMP2 or RAMP3 DNA. DNA lipid complexes were formed in 1 ml serum-free OPTIMEM1 (Invitrogen, Carlsbad, CA) using 1.6 µg of human secretin receptor and 11.4 µg of human RAMPs or pcDNA3.1 as mock control, along with 60 µl of Lipofectamine 2000 (Invitrogen, Carlsbad, CA). After 45 min, DNA-lipid complexes were added to flasks of cells already containing 4 ml of serum-free OPTI-MEM1. The cells were left to be transfected overnight or for 15 h. Cells were then recovered for 8 h in complete medium and subsequently passaged and seeded into 96-well plates and 25 cm<sup>2</sup> culture flasks to achieve 60-90 % confluency for use the following day in functional assays.

### Confocal fluorescence microscopy

Possible RAMP association with GPCRs was studied in a morphologic translocation assay in which fluorescent RAMP was evaluated for movement from the endoplasmic reticulum to the plasma membrane. In this assay, COS cells were transiently transfected with both the RAMP and GPCR constructs. After 24 h, the cells were seeded onto UV-sterilized 25-mm coverslips, washed with phosphate-buffered saline (PBS) and fixed in 2 % (w/v) paraformaldehyde (in PBS) for 30 min at room temperature. Cells were then washed with PBS before being mounted on a microscope slide using vectashield. YFP fluorescence was observed using a Zeiss LSM 510 confocal microscope (Thornwood, NY) with excitation, 488 nm argon laser; emission, LP505 filter; pinhole diameter 2.6 airy units, Plan-Apochromat 63X/1.4NA oil. Background-subtracted images were collected and assembled using Adobe Photoshop 7.0 (Mountain View, CA). Fluorescent labeling of secretin receptors on receptor-expressing cells were carried out by incubating the cells with 50 nM secretin(1-27)-Gly-Cys- Alexa<sup>488</sup> (Alexa-secretin) (19) in PBS containing 0.08mM CaCl<sub>2</sub> and 0.1 mM MgCl<sub>2</sub> at 4°C for 90 min. After the incubation, the cells were washed twice with ice-cold PBS and fixed with 2% paraformaldehyde prior to being mounted on a slide using vectashield. The Alexa fluorescence was observed using an epifluorescence Zeiss microscope with an FITC filter set (excitation, 480/20 nm; dichroic mirror, Q515 lp; and emission, 535/30 nm).

### BRET studies

Molecular associations were further evaluated using a bioluminescence resonance energy transfer (BRET) assay. In this, measurements were performed with a suspension of approximately 25,000 COS cells expressing relevant fluorescently-tagged constructs in 96-well white Optiplates, as described previously (17). The measurements were initiated by adding the cell-permeant *Renilla* luciferase-specific substrate, coelenterazine *h* (Biotium, Hayward, CA), to achieve a final concentration of 5 µM. The resultant BRET signals were collected using the 2103 Envision fluorescence plate reader (PerkinElmer, Wellesley, MA) set up with the <700 nm mirror and with emission filter sets for luminescence (460 nm, bandwidth 25 nm) and fluorescence (535 nm, bandwidth 25 nm). The BRET ratios were calculated based on the ratio of emissions, as described previously (17).

Saturation BRET experiments were performed for validation of the BRET signals, as described previously (17). Here, COS cells were transfected with a constant amount of donor construct (Rlu-tagged construct at 1.0  $\mu\text{g}$  DNA/dish) and with increasing amounts of acceptor construct (YFP-tagged construct, ranging from 0.3  $\mu\text{g}$  to 6  $\mu\text{g}$  DNA/dish). BRET assays were performed 48 h after transfection. The BRET data were analyzed and were evaluated for quality-of-fit based on  $R^2$  values using Prism 3.0 (GraphPad Software, San Diego, CA).

### **Bimolecular fluorescence complementation**

Bimolecular fluorescence complementation assays were carried out in COS cells transiently expressing YN- and YC-tagged constructs. The COS cells were transfected with equimolar concentrations of YN-tagged secretin receptor and YC-tagged RAMP3 constructs. Twenty four hr after transfection, the cells were lifted using 0.05 % trypsin and were plated onto UV-sterilized cover slips and allowed to grow for 48 h before being fixed and mounted on a microscopic slide for fluorescence microscopy using standard YFP settings, as described above.

### **Functional assays**

Cells were harvested 16 h after transfection and seeded for use in cAMP, ERK1/2 phosphorylation, and calcium mobilization assays, or for antibody-binding experiments. Cells were allowed to adhere for 16 h, followed by serum-starvation for an additional 24 h prior to use in the functional assays.

### **Measurement of cAMP**

Intracellular cAMP levels were determined using either AlphaScreen methodology with Fusion plate reader (PerkinElmer, Wellesley, MA) (20) or LANCE methods with Envision plate reader (PerkinElmer) (17), as have been fully described and validated in the respective laboratories previously. Each data point was assayed in duplicate, and the quantity of cAMP generated was calculated from the raw data using a cAMP standard curve. Results are expressed as the means  $\pm$  S.E.M. of data from three independent experiments.

### **Calcium mobilization assay**

Transfected cells were seeded in poly-L-lysine-coated 96-well plates at a density of 50,000 cells/well, incubated overnight and serum-starved for an additional 24 h. Cells were washed three times with a modified Hanks buffered-saline solution (HBSS) (containing (in mM): NaCl, 150; KCl, 2.6;  $\text{MgCl}_2$ , 1.18; D-glucose, 10; HEPES, 10;  $\text{CaCl}_2$ , 2.2; probenecid, 2 and 0.5 % (w/v) BSA. In light-diminished conditions, 100  $\mu\text{l}$  of wash solution was added containing the cell-permeant calcium fluorophore, Fluo-4/AM (10  $\mu\text{M}$ ) and incubated for 1 h at 37  $^\circ\text{C}$ . The fluorophore solution was aspirated from the wells, and cells were washed twice then incubated for 30 min in modified HBSS at 37  $^\circ\text{C}$ . The assay plate was transferred to a FlexStation (Molecular Devices, Palo Alto, CA), which performed the robotic addition of ligands (10  $\times$  stocks in modified HBSS). Receptor-mediated changes in intracellular calcium concentration were immediately recorded by the FlexStation using an excitation wavelength of 485 nm and emission wavelength of 520 nm. Data were collected for each well every 1.52 s for a total of 135 s.

### **ERK1/2 phosphorylation assay**

Transfected cells were seeded in 96-well plates at a density of 50,000 cells/well, and incubated for 16 h prior to being serum-starved overnight. On the day of assay, cells were pre-treated with buffer or inhibitors (at the concentrations specified) and then stimulated with agonist at 37  $^\circ\text{C}$ . Time-course results demonstrated a peak response at 10 min for all receptor complexes following agonist stimulation; this time point was subsequently used in concentration-response

studies. ERK1/2 phosphorylation was measured using the AlphaScreen-based ERK1/2 SureFire assay kit as previously described (21). Data are expressed as the percent response relative to stimulation with 10 % FBS.

### **Determination of cell-surface expression of receptors using enzyme-linked immunosorbent assay**

COS and CHO-K1 cells were transfected as described above. All receptor constructs incorporated a myc epitope tag at the amino terminus, which enabled cell-surface expression to be determined by enzyme-linked immunosorbent assay as described previously (22). Results were normalized against data from non-transfected cells. All experiments were performed in quadruplicate.

### **Internalization assay**

Cells transfected with myc-secretin receptor, RAMPs, NSF or NHERF1 were used for an enzyme-linked immunosorbent assay-based internalization assay in which the surface expression of the secretin receptor was assessed at 1, 2, 3, 4, 6, 8, 10 s and then at 5 min intervals for 60 min after exposure to 100 nM secretin. Internalization profiles of cells transfected with myc-secretin and RAMPs were compared in the presence or absence of either NSF or NHERF1.

### **Data Analysis**

cAMP, ERK1/2 phosphorylation, and calcium mobilization concentration-response data were analyzed via nonlinear regression using PRISM version 5 (GraphPad Software, San Diego, CA). In all instances, data points are shown as the mean  $\pm$  S.E.M.

## **RESULTS**

### **Cellular translocation assay for possible interactions between RAMPs and the secretin receptor**

The classical assay for RAMP association with a GPCR involves the demonstration of the ability of the receptor to translocate the fluorescent RAMP from the biosynthetic compartment to the plasma membrane (4,7). We performed this assay with COS cells transiently expressing fluorescent RAMPs and the secretin receptor, using CLR (known to associate with all three RAMPs) as a positive control. Shown in Figure 1 are COS cells transfected with YFP-tagged RAMP constructs in the absence or presence of GPCR constructs. In the absence of receptor co-transfection (left column), the fluorescent RAMPs all remained in the biosynthetic compartments, particularly the endoplasmic reticulum. Following, co-transfection with CLR (right column), the fluorescent RAMP signals were clearly observed at the plasma membrane, demonstrating the known effect of association between the RAMPs and that receptor. Analogous experiments with the secretin receptor (middle column) generated a similar fluorescence signal at the plasma membrane for RAMP3, but none for RAMP1 or RAMP2. This suggests that the secretin receptor can interact in a structurally-specific manner with RAMP3. This had not previously been observed or reported.

### **BRET studies of possible RAMP interactions with the secretin receptor**

We also utilized resonance energy transfer studies to examine the possible interactions between RAMPs and the secretin receptor (Fig 2A). In these studies, Rlu-tagged secretin receptor was used as donor and YFP-tagged RAMP constructs were used as possible acceptors. The well-established interactions between the calcitonin receptor and all three RAMPs (3) were used as positive controls in this series of studies. Indeed, in this assay, the calcitonin receptor expressed with RAMP1, RAMP2, or RAMP3 each generated a strong BRET signal above background;

the latter established by the co-expression of RAMP-Rlu with cytosolic YFP. Of note, a similar positive BRET signal was generated by the co-expression of the secretin receptor with RAMP3. In contrast, the secretin receptor co-expressed with RAMP1 or RAMP2 did not produce a significant BRET signal above background. These data confirm the apparent structurally-significant interaction between the family B G protein-coupled secretin receptor and RAMP3 that was suggested by the cellular translocation assay data.

The static BRET assay results were further validated using saturation BRET studies. Saturation BRET studies were performed to distinguish a specific and saturable molecular interaction between the secretin receptor and RAMP3, in contrast to a random molecular association between the donor and acceptor in a crowded cellular compartment. Figure 2B shows the BRET signals typical of a specific interaction in COS cells expressing a fixed concentration of donor construct (SecR-Rlu) with increasing amounts of acceptor construct (RAMP3-YFP), with the BRET signal increasing and then reaching a plateau. This was similar to the positive control that was generated when the calcitonin receptor was co-expressed with RAMP1, RAMP2, or RAMP3. In contrast, the BRET signals reflecting possible secretin receptor interaction with RAMP1 were not different from a linear fit through the origin, as is typical of a non-specific interaction.

The agonist-dependency of the interaction between the secretin receptor and RAMP3 was also studied using an analogous BRET assay (Fig 2C). There was no significant effect of ligand occupation on the signal in this assay using stimulation with secretin concentrations as high as 1  $\mu$ M.

### **Bimolecular fluorescence complementation to demonstrate secretin receptor-RAMP3 interactions**

The bimolecular fluorescence complementation approach was used to further demonstrate the specific interaction between the secretin receptor and RAMP3 (Fig 3). RAMP3-YFP expressed in the absence of receptor transfection was observed to reside in cellular biosynthetic compartments, particularly the endoplasmic reticulum. When RAMP3 was tagged with YN or YC, no fluorescence was observed. However, when RAMP-YN and RAMP-YC were co-expressed, the fluorescence pattern was similar to that of RAMP3-YFP, consistent with the ability of RAMP molecules to dimerize, as has been reported (3), yet this signal was limited to the intracellular biosynthetic compartments. When the non-fluorescent SecR-YN construct was co-expressed with the RAMP3-YC construct, a fluorescent signal was observed at the level of the plasma membrane. This pattern of response was similar to that observed when analogous studies were performed with the known RAMP3 partner, the calcitonin receptor, representing a positive control for this assay.

### **Exploring the region of the secretin receptor that contributes to its interaction with RAMP3**

To explore the molecular basis for the interaction between the secretin receptor and RAMP3, BRET and cellular translocation studies were performed with truncated receptor constructs. In the static and saturation BRET studies, secretin receptor constructs with truncation of the amino-terminal region (residues 1-121) or truncation of the carboxyl-terminal region (residues 376-419) displayed similar levels of energy transfer to those observed with the intact wild type secretin receptor, suggesting that the terminal regions were not critical for RAMP association with this receptor (Fig 4A and 4B). Morphological translocation studies of fluorescently-tagged RAMP3 were also consistent with the BRET data (Fig 5).

The possible contribution of the transmembrane (TM) helical bundle region of the secretin receptor to its interaction with RAMP3 was explored using a different experimental strategy. In this, peptides representing each of the TM segments were used to compete for a critical

epitope in the bimolecular fluorescence complementation assay with YN-tagged RAMP3 and YC-tagged secretin receptor that normally yields fluorescence at the level of the plasma membrane. When a critical epitope for interaction between the secretin receptor and RAMP3 would be delivered to this system, the plasma membrane fluorescence would be expected to be reduced or eliminated. Indeed, as observed in Figure 6, this was the case for the peptides encompassing TM6 and TM7. Each of the other secretin receptor TM segment peptides elicited no competitive disruption of this signal.

To further confirm these observations, receptor chimeras were created between the GLP1 receptor that is known to not associate with any RAMP (7), and the secretin receptor. These chimeric receptor constructs trafficked normally and were structurally and functionally intact, as reflected by their abilities to bind and signal in response to secretin. The following concentrations of secretin (nM) were able to stimulate half-maximal cAMP responses in COS cells expressing the respective constructs, as determined by the LANCE methodology (17): SecR,  $0.4 \pm 0.15$ ; Sec(GLP1<sub>TM1-3</sub>)R,  $4.4 \pm 0.12$ ; Sec(GLP1<sub>TM4-5</sub>)R,  $5.9 \pm 1.84$ ; and Sec(GLP1<sub>TM6-7</sub>)R,  $6.8 \pm 1.1$ . Basal levels of cAMP in these cells were  $2.1 \pm 0.5$  picomoles per million cells, while maximal levels achieved ( $E_{max}$  values) represented the following for each construct were: SecR,  $178 \pm 24$ ; Sec(GLP1<sub>TM1-3</sub>)R,  $153 \pm 14$ ; Sec(GLP1<sub>TM4-5</sub>)R,  $149 \pm 15$ ; and Sec(GLP1<sub>TM6-7</sub>)R,  $165 \pm 15$  picomoles per million cells. As predicted by the competitive TM peptide approach, only the chimeric constructs incorporating the secretin receptor TM6 and TM7 regions were able to translocate the fluorescent RAMP3 construct (Fig 7). The chimeric secretin receptors incorporating TM1-TM3 and TM4-TM5 regions of the GLP1 receptor behaved like the wild type secretin receptor, transporting the fluorescent RAMP3 construct to the cell surface. However, when the TM6-TM7 regions of the GLP1 receptor were included in the chimeric construct, this RAMP remained intracellularly in the biosynthetic compartment.

### Exploring the region of RAMP3 that contributes to its interaction with the secretin receptor

RAMP3 is a type I single transmembrane protein that has a large extracellular amino-terminal region and a very small intracellular carboxyl-terminal region. In this series of studies, most of the amino-terminal tail of RAMP3 was deleted (residues 10-100). This was studied in BRET and morphological translocation assays using YFP-tagged ( $\Delta 10-100$ )RAMP3 and Rlu-tagged secretin receptor in COS cells. Figures 8A and 8B show that this RAMP3 deletion construct behaved like wild type RAMP3, suggesting that the amino terminus does not contribute significantly to the molecular association. This was further supported by the morphologic translocation assay where ( $\Delta 10-100$ )RAMP3 retained the ability to translocate to the cell surface when co-expressed with the secretin receptor (Fig 8C).

### Functional assays

RAMP-receptor interaction, in a receptor-specific and RAMP-specific manner, has been proposed to alter ligand recognition (4,6), signal strength and preference (7,23) and receptor internalization and recycling (24,25). We therefore sought to determine if interaction of RAMP3 with the secretin receptor could alter gross receptor function in signaling and internalization assays, in two cellular backgrounds (COS and CHO-K1 cells). It must be remembered, however, that the secretin receptor is capable of trafficking normally to the plasma membrane even in the absence of RAMPs. Thus, unlike the early functional assays using CLR where only RAMP-associated receptor reaches the plasma membrane, here RAMP-free and RAMP3-associated secretin receptor are present on the cell surface. In COS cells, RAMP3 co-expression did not alter secretin-induced increases in cAMP production, intracellular calcium mobilization, or phosphorylation of ERK1/2 (Table 1). Similarly, transient co-expression of the secretin receptor with each individual RAMP failed to elicit any specific change in these parameters, except for RAMP1 where a decrease in secretin potency in the COS cell cAMP assay was observed (Table 1) (20). No difference in intracellular calcium

mobilization or cAMP response was observed in CHO-K1 cells upon co-transfection with any of the RAMPs (Table 1). The lack of consistent effect by RAMP1 on cAMP response across the two cellular backgrounds suggests that the effect in COS cells is a nonspecific response of these cells, potentially via altered  $G_{\alpha s}$  levels. We further monitored internalization of myc-tagged secretin receptor in response to 100 nM secretin peptide. In CHO-K1 cells expressing the secretin receptor alone, secretin induced a rapid internalization of the receptor, with a  $t_{1/2}$  of ~1.5 min. Co-expression of individual RAMPs did not alter the rate or extent of receptor internalization (Fig 9A). Furthermore, additional co-expression of either NSF, or NHERF1, which modify the internalization or recycling of the RAMP3-based adrenomedullin 2 receptor (24,25), failed to affect secretin receptor internalization, either alone or in the presence of RAMP3 (Fig 9B,C). Cell surface expression of the myc-tagged secretin receptor, as determined by enzyme-linked immunosorbent assay, was not significantly different between receptor expressed alone or receptor expressed in the presence of RAMPs (data not shown).

Additional studies were performed to further explore potential function of the RAMP3-secretin receptor association. In the first series of these studies, a secretin receptor mutant in which Gly<sup>241</sup> in TM4 was replaced with Cys (G241C), resulting in a receptor mutant that did not traffick normally to the plasma membrane. This construct was trapped in the biosynthetic machinery, likely the endoplasmic reticulum (26). In the presence of RAMP3, this defect was partially corrected, resulting in more receptor trafficking to the plasma membrane and the emergence of demonstrable biological activity in response to secretin stimulation in intact cells (Fig 10). Furthermore, the transfection of increasing amounts of the secretin receptor along with constant amounts of CLR and RAMP3 resulted in attenuation of the adrenomedullin response (Fig 11), with a parallel loss of CLR at the cell surface as monitored by ELISA (data not shown). This suggests that the secretin receptor was able to compete with CLR for RAMP3, resulting in less CLR-RAMP3 adrenomedullin receptor complex at the cell surface.

## DISCUSSION

RAMPs were first discovered based on their function in an expression cloning strategy, seeking a calcitonin gene-related peptide (CGRP) receptor (4). It ultimately became clear that an accessory protein was necessary to be combined with the calcitonin receptor-like receptor (CLR) to facilitate its glycosylation and trafficking to the cell surface where it could bind and be activated by CGRP. This accessory protein was the first RAMP. This same type of survey was subsequently successful in identifying RAMP partners for the calcitonin receptor (CTR) and for the CLR, to provide molecular complexes that respond to amylin or adrenomedullin as well.

With both of these early recognized RAMP partners identified as family B GPCRs, many other members of the family have been screened for RAMP association. This was largely dependent on a fluorescent RAMP translocation assay in which receptor interaction with the RAMP, in transit through the biosynthetic compartments, leads to translocation of the RAMP to the plasma membrane. Indeed, this approach has been successful in demonstrating RAMP- and receptor-specific interactions where the PTH1, PTH2, VPAC1, and glucagon receptors all associate with one or more RAMPs, while the VPAC2, GHRH, GLP1 and GLP2 receptors do not appear to associate with any RAMPs (7,8). More recently, association of RAMP1 and RAMP3 with the calcium-sensing receptor has been reported (8). Despite this growing list of RAMP-receptor interactions, relatively little is known regarding the molecular mechanism(s) underlying the interaction. In the current study, we have identified the secretin receptor as a novel, specific partner for RAMP3 and have elucidated the interaction interface as TM6 and TM7 of the receptor.

To date, the best studied RAMP-GPCR interaction is that of CLR and RAMP1. For this receptor, a major component of the interaction interface is believed to be the amino-terminal domain of the receptor. Both the isolated amino-terminal domain of RAMP1 and the amino-terminal domain of RAMP1 linked to platelet-derived growth factor (PDGF) receptor transmembrane region are capable of eliciting cell surface expression of CLR and to engender a CGRP receptor phenotype (27). This is further supported by loss of cell surface expression of CLR following mutagenesis of specific aromatic amino acids in helix 3 of the RAMP1 amino terminus (1,2). A similar interaction between CLR and RAMP2 and RAMP3 is also likely as mutation of conserved amino-terminal histidine residues in these proteins also disrupts the ability of RAMPs and CLR to translocate to the cell surface, although the specific role of individual histidines can differ between RAMPs (28). Nonetheless, the RAMP transmembrane region also played a contributory role in the interaction with CLR with both the isolated amino-terminal domain and the RAMP1-PDGF receptor chimera unable to fully reconstitute RAMP1 function (27).

The critical role of the amino-terminal domains of CLR and the RAMPs contrasts with the lack of importance of these domains for interaction between the secretin receptor and RAMP3 observed in the current study. Deletion of either the secretin receptor amino terminus or the RAMP3 amino terminus had little effect on trafficking of RAMP3 to the cell surface. Use of isolated receptor transmembrane peptides and chimeras between the secretin receptor and the GLP1 receptor refined the key site of interaction to TM6 and TM7. A key role for the transmembrane region of RAMPs in receptor interaction has also been observed for the CTR where chimeras of RAMP1 and RAMP2 implicated the transmembrane region as the key determinant of the difference in strength of induction of amylin receptor phenotype (29,30), however, the site of this interaction within the CTR has not been determined.

Phenotypically, all GPCR-RAMP interactions identified to date enable cell surface translocation of intracellularly retained RAMPs, which is not surprising as this is the underlying tenet for most assays for interaction. However, despite their initial description as modulators of peptide-binding specificity in association with CLR (4), the alteration of binding profiles has only been observed for CLR and the closely-related CTR (1,2). For other interacting receptors, including the VPAC1 and PTH1 receptor, no effect on peptide affinity has been observed (7). A similar lack of effect by RAMP3 on secretin interaction with its receptor was found in the current study, with no apparent change in secretin potency across a broad range of assays including cAMP accumulation, intracellular calcium mobilization and phosphorylation of ERK1/2.

As with most receptors, the secretin receptor does not require RAMP co-expression for cell surface expression. Therefore, we cannot rule out the possibility that the lack of a specific demonstrable signaling phenotype in these assays is due to the expression of “uncomplexed” secretin receptor at the cell surface that overwhelms the response of RAMP3-secretin receptor complexes, since the percentage of complexed and uncomplexed receptor is unknown. However, under the varying conditions of assay for BRET and bimolecular fluorescence complementation, the level of interaction between RAMP3 and the secretin receptor was similar to that seen for CLR or CTR interaction with RAMP3, the classic RAMP-associating receptors. For the CTR, this level of interaction clearly enables resolution of signaling from uncomplexed and complexed receptor despite a high level of background uncomplexed CTR phenotype (6,23,29,31).

Functional consequence of the secretin receptor-RAMP3 interaction was demonstrated in two additional assays. In the first series of studies, a trafficking-defective secretin receptor mutant was rescued by RAMP3 co-expression. This suggests that the RAMP can play a chaperone-like role for an interacting receptor, even when this is not required for routine cell surface

receptor expression. In the second series of studies, secretin receptor competed for the RAMP3 interaction with CLR, an interaction that is critical for the establishment of a functional adrenomedullin receptor. Thus, we also need to be cognizant of how interacting molecules might saturate and compete for other functionally-important molecular associations.

The lack of effect in modulation of apparent secretin affinity is consistent with the lack of interaction between the amino-terminal domains of the secretin receptor and RAMP3. Indeed, it implies that lack of significant association between the amino-terminal domains may be the norm rather than the exception for most family B GPCR-RAMP interactions. The identification of TM6 and TM7 as the secretin-RAMP3 interface is therefore the first mechanistic guide to how most RAMP-family B receptor associations may occur.

Of note, the RAMP-secretin receptor interface is distinct from the homodimerization interface for secretin receptors that we recently identified as TM4 of this receptor (17).

Homodimerization of the secretin receptor appears to be important for efficient signaling of the receptor (17), and our current data are consistent with an ability of RAMP3 to interact with an intact secretin receptor homodimer. For the CLR, elegant work has revealed that it is also a homodimer of this receptor that interacts with RAMPs, with the RAMP present as a monomer (32), although the final stoichiometry of the complex is not clear. Assuming that there is conservation of function across family B GPCRs, these data provide support for the potential extrapolation of our current findings as a model for RAMP-family B GPCR transmembrane region interactions, however, an alternate interface involving TM1 and TM2 of CLR cannot be ruled out.

The other key RAMP-dependent phenotype that has been observed for CLR-RAMP3 interactions is an alteration to adrenomedullin-induced internalization and recycling of the AM<sub>2</sub> receptor (24,25). The AM<sub>2</sub> receptor, but not the RAMP2-associated AM<sub>1</sub> receptor, may be alternatively targeted for lysosomal degradation, rapidly recycled or not internalized at all depending upon interaction of the carboxyl-terminal RAMP3 PDZ domain with either NSF or NHERF1. Consequently, we studied internalization of the secretin receptor in the presence and absence of RAMPs and also in the context of overexpression of either NSF or NHERF1. However, internalization of the secretin receptor was not altered by RAMP3, either alone or in the presence of NSF or NHERF1, suggesting that the protein-protein interactions engendered by RAMP3 are contextual on the presentation of the PDZ epitope by its receptor partner.

The resolution of the site of transmembrane interaction between RAMP3 and the secretin receptor provides impetus towards understanding the molecular basis for the specificity of RAMP-GPCR interactions. If this interaction interface is confirmed for other GPCRs, it will enable a bioinformatic approach to prediction of RAMP-GPCR interactions. For example, the secretin receptor and the PTH2 receptor specifically interact with RAMP3, while the PTH1 and glucagon receptors specifically interact with RAMP2. There has been substantial work to explore the molecular basis of helix-helix interactions within the lipid bilayer (33-35). Within the helical domain of the three RAMPs, there is approximately 30 percent identity of the amino acid residues and 60 percent homology. The differences between the RAMPs should be adequate to explain the specificity of interaction between a given GPCR and a given RAMP. Conservation of the site of transmembrane interaction would therefore allow rules to be developed for predicting such interactions.

Our data also provides further evidence for complexity in the functional consequence of RAMP-GPCR interaction with existing phenotypes varying greatly across interacting receptors and also many examples of lack of understanding of the functional significance of RAMP-GPCR interaction, as currently is the case for the secretin receptor-RAMP3 interaction. The

broad distribution of RAMPs suggests that substantial work is still required to fully understand their role in physiology and disease.

## Supplementary Material

Refer to Web version on PubMed Central for supplementary material.

## Acknowledgments

The authors thank Mary Lou Augustine and Alicja Skalecka Ball (Mayo Clinic) for their excellent technical assistance. We also thank Maria M. Morfis (Monash University) for preparing the Rlu- and YFP-tagged RAMP constructs.

## The abbreviations used are the following

BRET	bioluminescence resonance energy transfer
CGRP	calcitonin gene-related peptide
CLR	calcitonin receptor-like receptor
CTR	calcitonin receptor
DMEM	Dulbecco's modified Eagle's medium
GHRH	growth hormone releasing hormone
GPCR	G protein-coupled receptor
GLP	glucagon-like peptide
KRH	Krebs-Ringer-HEPES
NHERF1	sodium-hydrogen exchange regulatory factor
NSF	N-ethylmaleimide-sensitive factor
PBS	phosphate-buffered saline
PTH	parathyroid hormone
RAMPs	receptor activity-modifying proteins
Rlu	<i>Renilla</i> luciferase
SecR	human secretin receptor
VPAC	vasoactive intestinal polypeptide receptor
YFP	yellow fluorescent protein
YN	YFP(1-158)
YC	YFP(159-238).

## REFERENCES

1. Hay DL, Poyner DR, Sexton PM. GPCR modulation by RAMPs. *Pharmacol. Ther* 2006;109:173–197. [PubMed: 16111761]
2. Sexton PM, Poyner DR, Simms J, Christopoulos A, Hay DL. Modulating receptor function through RAMPs: can they represent drug targets in themselves? *Drug Discov. Today* 2009;14:413–419. [PubMed: 19150656]
3. Udawela M, Hay DL, Sexton PM. The receptor activity modifying protein family of G protein coupled receptor accessory proteins. *Semin. Cell Dev. Biol* 2004;15:299–308. [PubMed: 15125893]

4. McLatchie LM, Fraser NJ, Main MJ, Wise A, Brown J, Thompson N, Solari R, Lee MG, Foord SM. RAMPs regulate the transport and ligand specificity of the calcitonin-receptor-like receptor. *Nature* 1998;393:333–339. [PubMed: 9620797]
5. Born W, Fischer JA, Muff R. Receptors for calcitonin gene-related peptide, adrenomedullin, and amylin: the contributions of novel receptor-activity-modifying proteins. *Receptors Channels* 2002;8:201–209. [PubMed: 12529937]
6. Christopoulos G, Perry KJ, Morfis M, Tilakaratne N, Gao Y, Fraser NJ, Main MJ, Foord SM, Sexton PM. Multiple amylin receptors arise from receptor activity-modifying protein interaction with the calcitonin receptor gene product. *Mol. Pharmacol* 1999;56:235–242. [PubMed: 10385705]
7. Christopoulos A, Christopoulos G, Morfis M, Udawela M, Laburthe M, Couvineau A, Kuwasako K, Tilakaratne N, Sexton PM. Novel receptor partners and function of receptor activity-modifying proteins. *J. Biol. Chem* 2003;278:3293–3297. [PubMed: 12446722]
8. Morfis M, Christopoulos A, Sexton PM. RAMPs: 5 years on, where to now? *Trends Pharmacol. Sci* 2003;24:596–601. [PubMed: 14607083]
9. Bouschet T, Martin S, Henley JM. Receptor-activity-modifying proteins are required for forward trafficking of the calcium-sensing receptor to the plasma membrane. *J. Cell Sci* 2005;118:4709–4720. [PubMed: 16188935]
10. Ishihara T, Nakamura S, Kaziro Y, Takahashi T, Takahashi K, Nagata S. Molecular cloning and expression of a cDNA encoding the secretin receptor. *Embo J* 1991;10:1635–1641. [PubMed: 1646711]
11. Ulrich CD 2nd, Holtmann M, Miller LJ. Secretin and vasoactive intestinal peptide receptors: members of a unique family of G protein-coupled receptors. *Gastroenterology* 1998;114:382–397. [PubMed: 9453500]
12. Dong M, Lam PC, Gao F, Hosohata K, Pinon DI, Sexton PM, Abagyan R, Miller LJ. Molecular Approximations between Residues 21 and 23 of Secretin and Its Receptor: Development of a Model for Peptide Docking with the Amino Terminus of the Secretin Receptor. *Mol. Pharmacol* 2007;72:280–290. [PubMed: 17475809]
13. Dong M, Lam PC, Pinon DI, Sexton PM, Abagyan R, Miller LJ. Spatial approximation between secretin residue five and the third extracellular loop of its receptor provides new insight into the molecular basis of natural agonist binding. *Mol. Pharmacol* 2008;74:413–422. [PubMed: 18467541]
14. Harikumar KG, Happs RM, Miller LJ. Dimerization in the absence of higher-order oligomerization of the G protein-coupled secretin receptor. *Biochim. Biophys. Acta* 2008;1778:2555–2563. [PubMed: 18680717]
15. Harikumar KG, Morfis MM, Lisenbee CS, Sexton PM, Miller LJ. Constitutive formation of oligomeric complexes between family B G protein-coupled vasoactive intestinal polypeptide and secretin receptors. *Mol. Pharmacol* 2006;69:363–373. [PubMed: 16244179]
16. Harikumar KG, Morfis MM, Sexton PM, Miller LJ. Pattern of intra-family hetero-oligomerization involving the G-protein-coupled secretin receptor. *J. Mol. Neurosci* 2008;36:279–285. [PubMed: 18401761]
17. Harikumar KG, Pinon DI, Miller LJ. Transmembrane segment IV contributes a functionally important interface for oligomerization of the Class II G protein-coupled secretin receptor. *J. Biol. Chem* 2007;282:30363–30372. [PubMed: 17726027]
18. Lisenbee CS, Miller LJ. Secretin receptor oligomers form intracellularly during maturation through receptor core domains. *Biochemistry* 2006;45:8216–8226. [PubMed: 16819820]
19. Harikumar KG, Hosohata K, Pinon DI, Miller LJ. Use of probes with fluorescence indicator distributed throughout the pharmacophore to examine the peptide agonist-binding environment of the family B G protein-coupled secretin receptor. *J. Biol. Chem* 2006;281:2543–2550. [PubMed: 16319066]
20. Hay DL, Christopoulos G, Christopoulos A, Poyner DR, Sexton PM. Pharmacological discrimination of calcitonin receptor: receptor activity-modifying protein complexes. *Mol. Pharmacol* 2005;67:1655–1665. [PubMed: 15692146]
21. van der Westhuizen ET, Werry TD, Sexton PM, Summers RJ. The relaxin family peptide receptor 3 activates extracellular signal-regulated kinase 1/2 through a protein kinase C-dependent mechanism. *Mol. Pharmacol* 2007;71:1618–1629. [PubMed: 17351017]

22. Hawtin SR, Simms J, Conner M, Lawson Z, Parslow RA, Trim J, Sheppard A, Wheatley M. Charged extracellular residues, conserved throughout a G- protein-coupled receptor family, are required for ligand binding, receptor activation, and cell-surface expression. *J. Biol. Chem* 2006;281:38478–38488. [PubMed: 16990262]
23. Morfis M, Tilakaratne N, Furness SG, Christopoulos G, Werry TD, Christopoulos A, Sexton PM. Receptor activity-modifying proteins differentially modulate the G protein-coupling efficiency of amylin receptors. *Endocrinology* 2008;149:5423–5431. [PubMed: 18599553]
24. Bomberger JM, Parameswaran N, Hall CS, Aiyar N, Spielman WS. Novel function for receptor activity-modifying proteins (RAMPs) in post-endocytic receptor trafficking. *J. Biol. Chem* 2005;280:9297–9307. [PubMed: 15613468]
25. Bomberger JM, Spielman WS, Hall CS, Weinman EJ, Parameswaran N. Receptor activity-modifying protein (RAMP) isoform-specific regulation of adrenomedullin receptor trafficking by NHERF-1. *J. Biol. Chem* 2005;280:23926–23935. [PubMed: 15805108]
26. Gao F, Harikumar KG, Dong M, Lam PC, Sexton PM, Christopoulos A, Bordner A, Abagyan R, Miller LJ. Functional importance of a structurally distinct homodimeric complex of the family B G protein-coupled secretin receptor. *Mol. Pharmacol* 2009;76:264–274. [PubMed: 19429716]
27. Fitzsimmons TJ, Zhao X, Wank SA. The extracellular domain of receptor activity-modifying protein 1 is sufficient for calcitonin receptor-like receptor function. *J. Biol. Chem* 2003;278:14313–14320. [PubMed: 12574158]
28. Kuwasako K, Kitamura K, Nagata S, Kato J. Functions of the extracellular histidine residues of receptor activity-modifying proteins vary within adrenomedullin receptors. *Biochem. Biophys. Res. Commun* 2008;377:109–113. [PubMed: 18835256]
29. Udawela M, Christopoulos G, Morfis M, Christopoulos A, Ye S, Tilakaratne N, Sexton PM. A critical role for the short intracellular C terminus in receptor activity-modifying protein function. *Mol. Pharmacol* 2006;70:1750–1760. [PubMed: 16912219]
30. Zumpe ET, Tilakaratne N, Fraser NJ, Christopoulos G, Foord SM, Sexton PM. Multiple ramp domains are required for generation of amylin receptor phenotype from the calcitonin receptor gene product. *Biochem. Biophys. Res. Commun* 2000;267:368–372. [PubMed: 10623626]
31. Udawela M, Christopoulos G, Tilakaratne N, Christopoulos A, Albiston A, Sexton PM. Distinct receptor activity-modifying protein domains differentially modulate interaction with calcitonin receptors. *Mol. Pharmacol* 2006;69:1984–1989. [PubMed: 16531504]
32. Heroux M, Hogue M, Lemieux S, Bouvier M. Functional calcitonin gene-related peptide receptors are formed by the asymmetric assembly of a calcitonin receptor-like receptor homo-oligomer and a monomer of receptor activity-modifying protein-1. *J. Biol. Chem* 2007;282:31610–31620. [PubMed: 17785463]
33. Ben-Tal N, Honig B. Helix-helix interactions in lipid bilayers. *Biophys. J* 1996;71:3046–3050. [PubMed: 8968575]
34. Cuthbertson JM, Bond PJ, Sansom MS. Transmembrane helix-helix interactions: comparative simulations of the glycoporphin a dimer. *Biochemistry* 2006;45:14298–14310. [PubMed: 17128969]
35. Yohannan S, Faham S, Yang D, Whitelegge JP, Bowie JU. The evolution of transmembrane helix kinks and the structural diversity of G protein-coupled receptors. *Proc. Natl. Acad. Sci. U S A* 2004;101:959–963. [PubMed: 14732697]

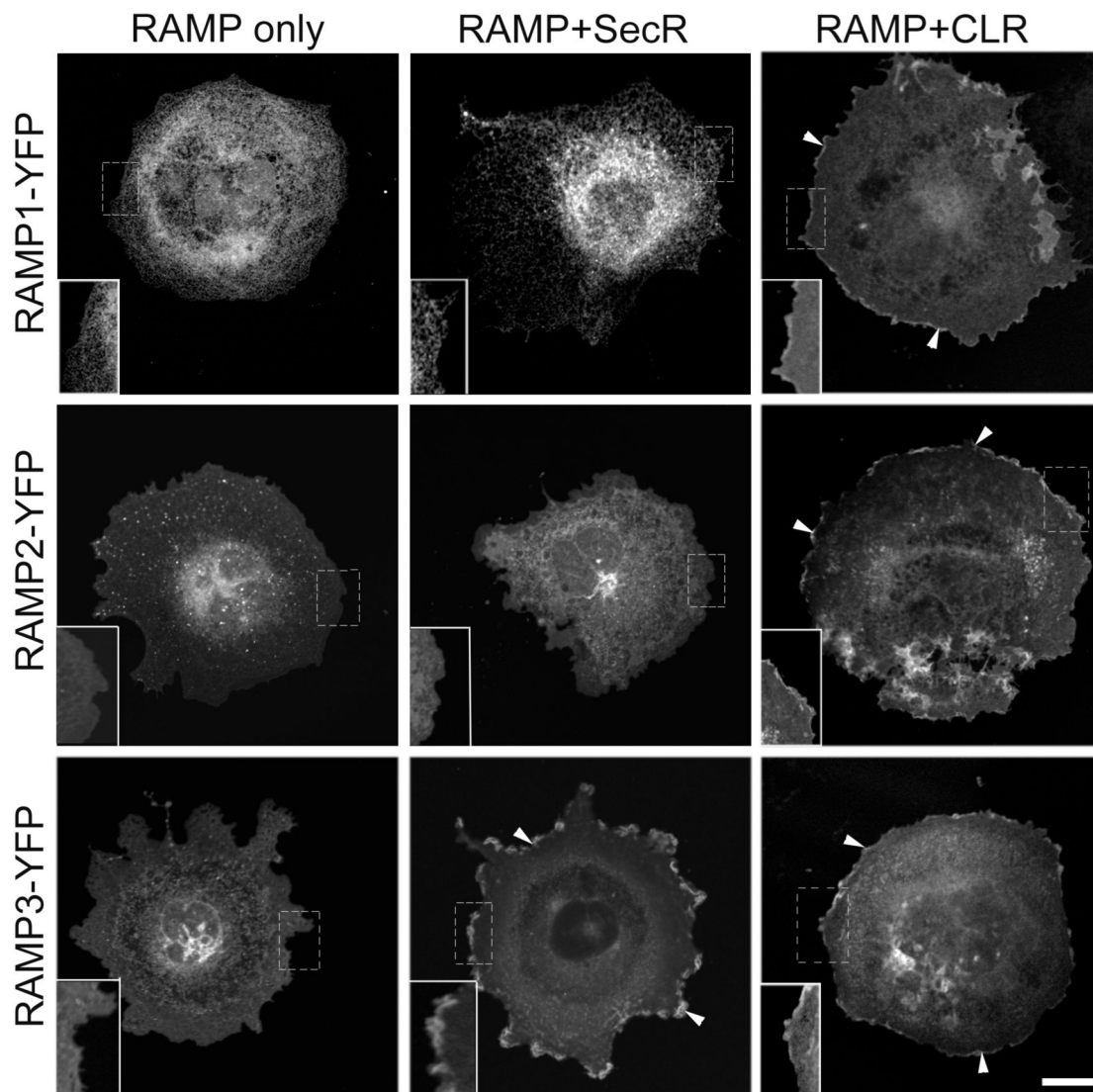


**FIGURE 1. Morphologic assays for RAMP translocation to the plasma membrane**

Shown are fluorescence images of the expression of each type of RAMP in COS cells, all localized to biosynthetic compartments, particularly representing the endoplasmic reticulum (left column). The right column shows the changes in distribution of the fluorescence when the calcitonin receptor-like receptor was co-expressed with each YFP-tagged RAMP. In all three conditions, there was significant translocation to the plasma membrane (highlighted with arrowheads). The middle column shows the changes in distribution of the fluorescence when the secretin receptor was co-expressed with each RAMP. Here, only RAMP3 distribution was changed, with significant translocation to the plasma membrane (highlighted with arrowheads). Insets show the boxed regions at higher magnification. The images shown are representative of four similar experiments. Bar 25  $\mu\text{m}$ .

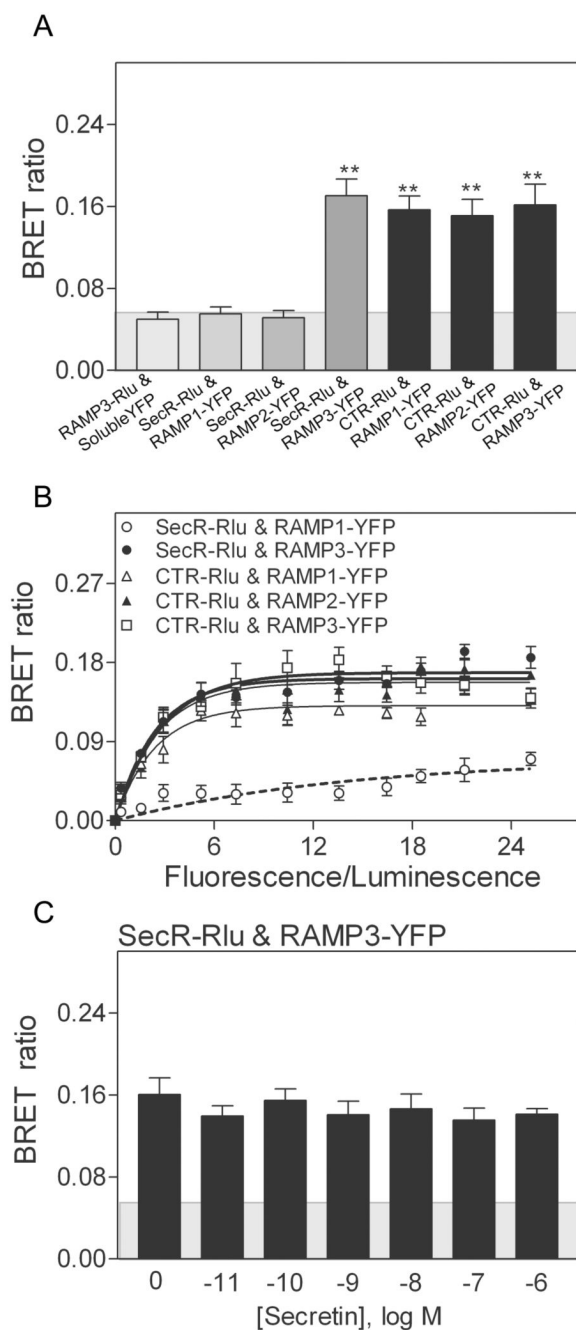


**FIGURE 2. BRET analysis of association between RAMPs and the secretin receptor**

Shown are BRET signals in static and saturation assays evaluating the potential interaction of the secretin receptor and RAMPs. In the static assays shown in panel A, background BRET signals were determined by expression of the Rlu-tagged RAMPs and soluble YFP. The co-expression of YFP-tagged RAMP1 and RAMP2 produced only background BRET. In contrast, co-expression of RAMP3 produced a significant BRET signal. This was similar to that produced by the positive control, the co-expression with the Rlu-tagged calcitonin receptor. Panel B shows the saturation BRET data, confirming the significance of the signal generated by co-expression of RAMP3 and the secretin receptor. In panel C, the effects of increasing concentrations of secretin on the BRET signal were studied. The cells were incubated with

specified concentrations of secretin at 37°C for 5 min before adding the coelenterazine *h* (5μM) to initiate the BRET signal. There was no significant effect of agonist on secretin receptor-RAMP3 interaction. The values plotted represent means ± S.E.M. of data from five independent experiments. \*\* p<0.001 significantly above background BRET signals.

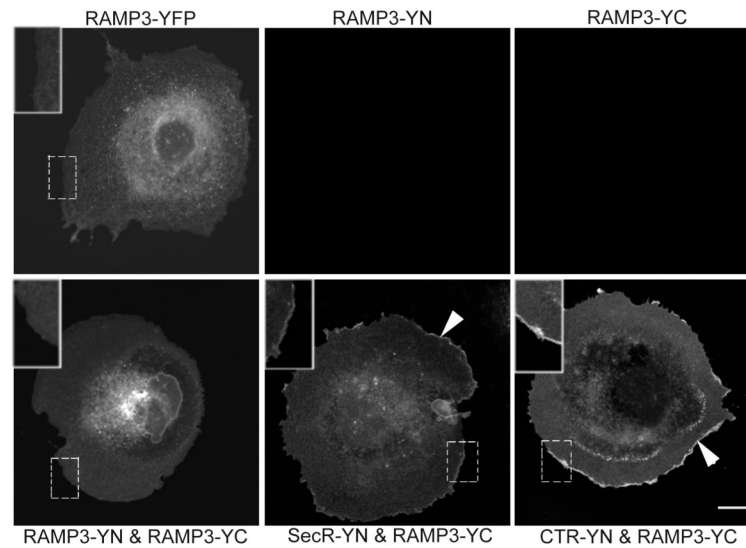


**FIGURE 3. Bimolecular fluorescence complementation assays**

Shown are typical fluorescence images of COS cells expressing the YFP-, YN-, and YC-tagged constructs, as noted. Significant fluorescence was noted at the cell surface (highlighted with arrowheads) when YC-tagged RAMP3 was co-expressed with the calcitonin receptor tagged with YN or with the secretin receptor tagged with YN. RAMP dimerization in the intracellular biosynthetic compartments was observed when RAMP-YN and RAMP-YC were co-expressed. Insets show the boxed regions at higher magnification. Bar 25  $\mu\text{m}$ .

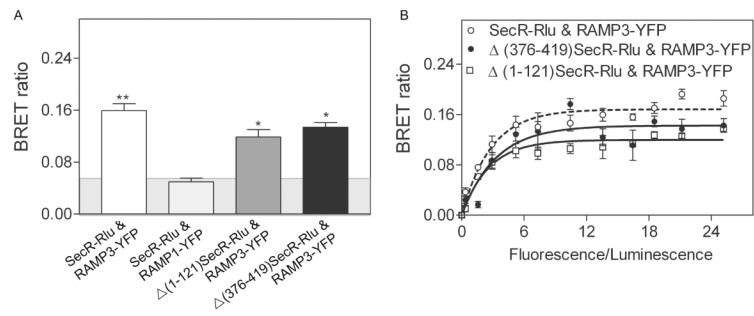


**FIGURE 4. BRET analysis of secretin receptor-RAMP3 interaction using truncated receptor constructs**

Shown are the static (A) and saturation (B) BRET signals obtained from COS cells coexpressing Rlu-tagged truncated secretin receptor with YFP-tagged RAMP3. Significant BRET signals above non-specific (shown in the *shaded area*) are marked \* $p < 0.01$ , \*\* $p < 0.001$ . The values plotted represent means  $\pm$  S.E.M. of data from five independent experiments.

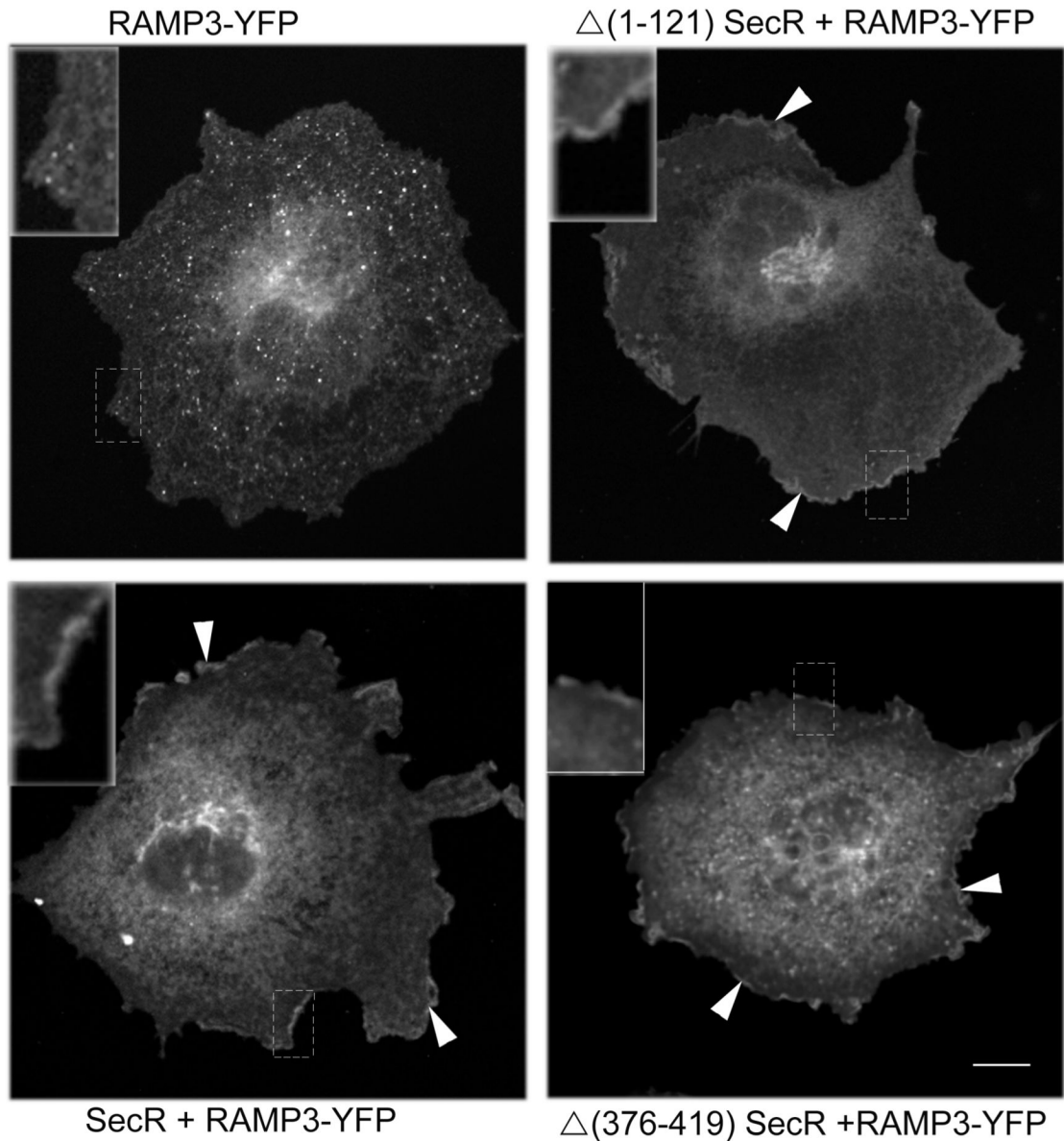


**FIGURE 5. Morphological RAMP translocation assay**

Shown are representative confocal microscopic images of COS cells expressing either YFP-tagged RAMPs alone or co-expressed with wild type or amino-terminal region ( $\Delta 1-121$ ) truncated or carboxyl-terminal region ( $\Delta 376-419$ ) truncated secretin receptor constructs. Each of the truncated secretin receptor constructs translocated the YFP-tagged RAMP3 to the cell surface (arrowheads) similar to wild type secretin receptor. These images shown are representative of four similar experiments. Insets show the boxed regions at higher magnification. Bar 25  $\mu\text{m}$ .

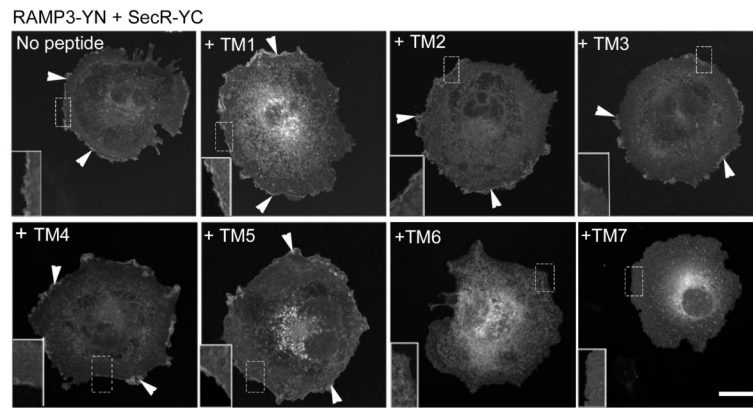


**FIGURE 6. Morphological bimolecular fluorescence complementation assay of RAMP3 interaction with the secretin receptor, determining the ability of transmembrane peptides to competitively disrupt the complex**

Shown are the representative confocal images of COS cells co-expressing YN-tagged RAMP3 and YC-tagged secretin receptor treated with or without the specified secretin receptor transmembrane peptides at a concentration of 40 $\mu$ g/ml for 2 hr prior to fixation of the cells. Cell surface fluorescence (highlighted with arrowheads) was competitively disrupted only by TM6 and TM7 peptides. Images shown are representative of images from three similar experiments. Insets show the boxed regions at higher magnification. Bar 25  $\mu$ m.

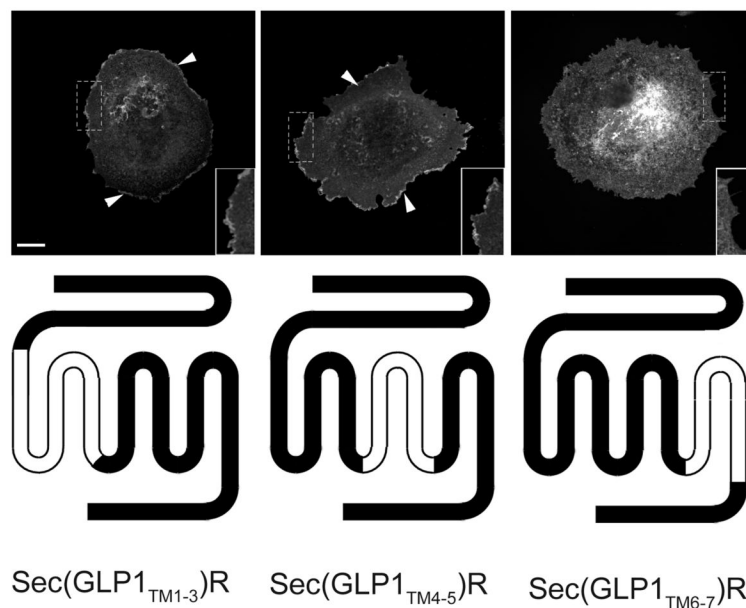


**FIGURE 7. Morphologic fluorescence analysis of chimeric receptor association with RAMP3**  
 Three chimeric secretin-GLP1 receptor constructs were studied for their abilities to translocate the fluorescent RAMP3 construct to the transfected COS cell surface. Sec(GLP1<sub>TM1-3</sub>)R and Sec(GLP1<sub>TM4-5</sub>)R behaved like wild type secretin receptor, associating with this RAMP and translocating it to the COS cell surface. However, Sec(GLP1<sub>TM6-7</sub>)R did not have this effect, behaving instead like the wild type GLP-1 receptor. This supports the interpretation that the TM6 and TM7 regions of the secretin receptor are responsible for its association with RAMP3. Insets show the boxed regions at higher magnification. Bar 25  $\mu$ m.

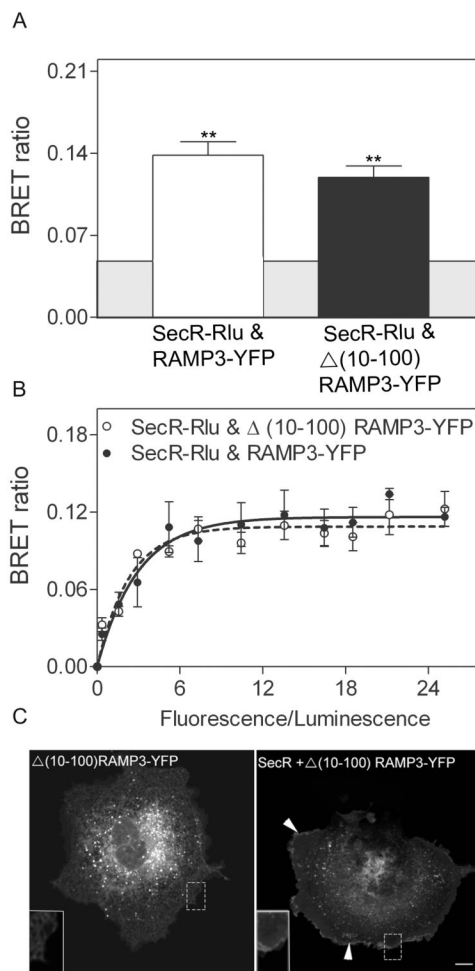


**FIGURE 8. BRET analysis of secretin receptor-RAMP3 interaction using the truncated RAMP3 construct**

Shown are the static (A) and saturation (B) BRET signals obtained from COS cells coexpressing Rlu-tagged secretin receptor with YFP-tagged amino-terminally-truncated RAMP3. Significant BRET signals above non-specific (shown in the *shaded area*) are marked  $**p < 0.001$ . The values plotted represent means  $\pm$  S.E.M. of data from five independent experiments. Also shown are representative images from morphological translocation assay (C). Confocal microscopic images were collected from COS cells coexpressing YFP-tagged truncated RAMP3 with untagged secretin receptor. The truncated RAMP3 was able to translocate the secretin receptor to the cell surface (arrowheads). The data marked  $**p < 0.001$  level in figure A represents significant BRET signal above the nonspecific signal shown in the *shaded area*. Insets show the boxed regions at higher magnification. The values plotted represent means  $\pm$  S.E.M. of data from five independent experiments. Bar 25  $\mu$ m.

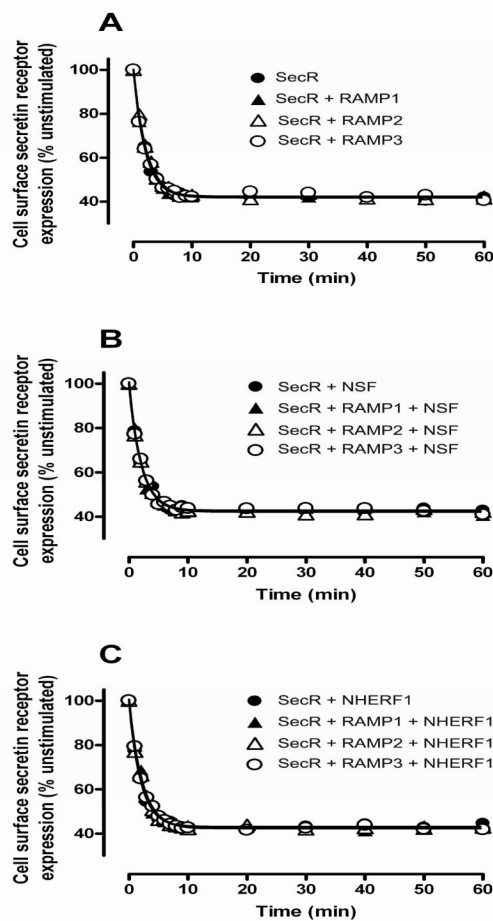


**FIGURE 9. Internalization of myc-tagged secretin receptor following stimulation with secretin peptide (100 nM)**

Shown is internalization of the secretin receptor in transiently-transfected CHO-K1 cells measured by loss of cell surface receptor expression in an anti-cmyc enzyme-linked immunosorbent assay. (A) secretin receptor internalization in the presence or absence of individual RAMPs, (B) secretin receptor internalization in the presence of NSF, in the presence or absence of individual RAMPs and (C) secretin receptor internalization, in the presence of NHERF1, in the presence or absence of individual RAMPs. The data plotted represent means  $\pm$  S.E.M. of data from three independent experiments. Where error bars are not visible these are contained within the plotted symbols. No RAMP3-specific alteration to responses was observed.

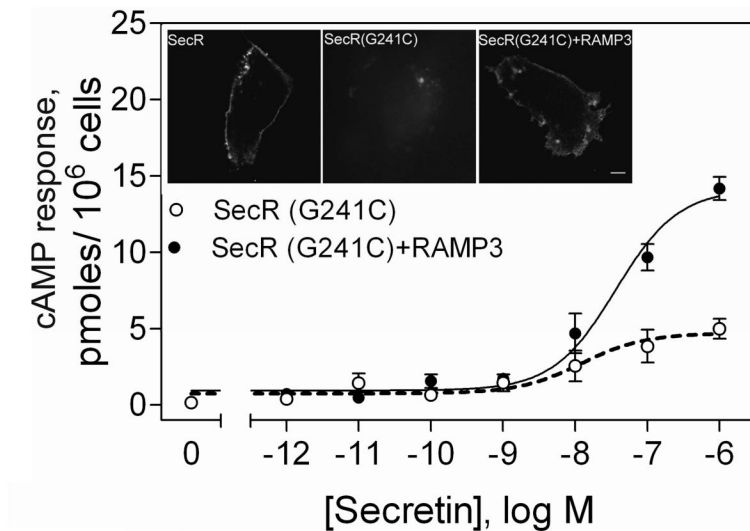


**FIGURE 10. Chaperone function of RAMP3 at a trafficking-defective secretin receptor mutant** Shown are cAMP concentration-response curves to secretin stimulation of intact COS cells expressing G241C secretin receptor mutant with or without RAMP3 (17). Shown in the inset are the microscopic images of Alexa-secretin-labeled cells showing the increased surface expression of the mutant receptor in the presence of RAMP3. The values plotted represent means  $\pm$  S.E.M. of data from three independent experiments. Bar 25  $\mu$ m.

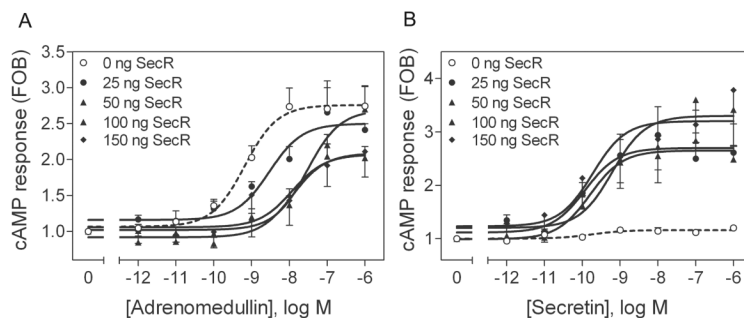


**FIGURE 11. Competitive inhibition of adrenomedullin action on the CLR-RAMP3 complex by secretin receptor expression**

Shown are cAMP responses to adrenomedullin (A) and secretin (B) in COS cells transfected with a fixed amount of myc-CLR (50 ng) and RAMP3 (100 ng), and increasing amounts of secretin receptor construct (noted for each curve). The values plotted represent means  $\pm$  S.E.M. of data from three or four independent experiments.

### TABLE 1 Impact of RAMP expression on secretin-stimulated biological responses at the secretin receptor

Shown are the responses to secretin in COS cells and CHO-K1 cells transiently expressing the myc-tagged secretin receptor either alone, or in the presence of individual RAMPs. Shown are cAMP (20), intracellular calcium, and phospho-ERK1/2 responses to secretin stimulation for 10 min. Values represent means±S.E.M. of data from three to five independent experiments. No significant RAMP3-induced changes were observed for any of the responses studied.

	$E_{C_{50}}$ (nM)					$E_{max}$ (cAMP, nM; $Ca^{2+}$ , RFU; ERK1/2, % FBS 10%)					
	SecR	+ RAMP1	SecR + RAMP2	+ RAMP3	SecR	+ RAMP1	SecR + RAMP2	+ RAMP3	SecR	+ RAMP2	+ RAMP3
<i>COS cells</i>											
cAMP	0.3±0.1	3.7±1.0*	0.3±0.1	0.2±0.2	3.392±154	4.477±162	4.466±55	4.026±283			
$Ca^{2+}$	2.4±1.0	2.4±0.1	0.8±0.1	1.0±0.1	33,404±151	35,598±166	36,261±133	36,082±134			
ERK1/2	3.6±1.0	2.0±0.1	2.4±1.0	2.3±1.0	40±0.2	44±0.2	44±0.2	47±0.2			
<i>CHO-K1 cells</i>											
cAMP	0.1±0.1	0.2±0.1	0.1±0.1	0.1±0.1	81±6	78±8	73±5	74±6			
$Ca^{2+}$	0.9±0.3	0.9±0.2	0.7±0.1	0.8±0.2	10,104±1,516	12,365±2,264	10,768±1,958	12,378±1,551			

\* Basal levels: In COS cells, cAMP: SecR 354±97, +RAMP1 932±53, +RAMP2 1182±34, +RAMP3 824±183;  $Ca^{2+}$ : SecR 343±158, +RAMP1 369±173, +RAMP2 487±163, +RAMP3 433±159; ERK1/2: SecR 0.43±0.19, +RAMP1 0.44±0.20, +RAMP2 0.44±0.20, +RAMP3 0.48±0.22. In CHO-K1 cells, cAMP: SecR 48±3, +RAMP1 47±2, +RAMP2 46±1, +RAMP3 48±5;  $Ca^{2+}$ : SecR 2976±1100, +RAMP1 1307±270, +RAMP2 1025±113, +RAMP3 1621±206.